ESCUELA DE CONSTRUCCIÓN CIVIL
FACULTAD DE INGENIERÍA

Revista de la Construcción
Journal of Construction

Research Article

Performance evaluation of steel-concrete composite structures designed in poorly graded soils

Serkan ETLİ [1]

[1] Department of Emergency Aid and Disaster Management, Munzur University, Tunceli (Turkey); serkanetli@munzur.edu.tr
*Correspondence: serkanetli@munzur.edu.tr

Received: 19.03.2022; **Accepted:** 25.04.2023; **Published:** 31.08.2023

Citation: Etli, S. (2023). Performance evaluation of steel-concrete composite structures designed in poorly graded soils. Revista de la Construcción. Journal of Construction, 22(2), 259-276. https://doi.org/10.7764/RDLC.22.2.259.

Abstract: In this study, the seismic behavior of steel concrete composite buildings in a specific region was investigated. For this purpose, 5-, 10-, 15- and 20-storey composite moment-resisting framed structures were designed. Moment-resisting composite framed structures are modeled with concrete-filled steel tube columns and designed and modeled using composite beams. The buildings are designed according to ÇYTHYE-2016 and TBEC-2018 regulations at design levels with high ductility. In the design of the designed structures, the peak ground acceleration value is 0.79 g, and the design ground is planned as ZE class. SeismoStruct software was used for the design and performance evaluation of the structures. During the performance evaluations of the structures, nonlinear static pushover and incremental dynamic analyzes were used. Uniform and triangular load distributions are adopted in the static pushover analysis and 16 earthquake ground motions are used in the incremental dynamic analysis. Evaluation of the effect of the number of stories on the earthquake behavior of composite moment-resisting framed structures was investigated using the non-linear analyzes mentioned. Accordingly, lateral response, overstrength factors, ductility, and dynamic behavior factor values for composite frame structures were calculated and presented using the relevant analysis results. It has been calculated that the behavior factor of all moment-resisting composite framed structures can perform well above the design assumptions, whereas moment-resistant composite framed structures absorb seismic energy by using inelastic deformations. Ductility is almost 30% higher than the design assumption for international standards. As a result, it was concluded that these structures could continue to serve theoretically.

Keywords: Composite moment resisting frame, concrete filled steel tube column, incremental dynamic analysis, nonlinear pushover analysis, seismic behavior factor.

1. Introduction

With the increase in the design heights of the buildings, the need for the use of columns with high strength capacities increases, especially to absorb the effects of earthquakes (Elghazouli, Castro, and Izzuddin 2008; Khosravi, H., Shoaib Mousavi, S., Tadayonfar 2020). For steel structures, high strength in columns can be achieved by using steel material class with high yield strength and/or profiles selected as larger cross-sections. On the other hand, in reinforced concrete structures, higher capacity columns can be obtained by increasing the class and/or compressive strength of the concrete material used and by increasing the cross section. In addition, it is possible to benefit from the high yield strength of steel and the high compressive strength of concrete by creating a single section to be obtained. Among the sections that can be produced in this

way, concrete-filled steel tube (CFST) sections, which are the most used and experimentally/theoretically studied in the last century, are the most used column elements (Shams and Saadeghvaziri 1997; Shanmugam and Lakshmi 2001).

The strength of columns, which are vertical load members in both steel and reinforced concrete structures, can be increased by designs that can be made using resultant sections without using relatively large cross-sectional areas. In other words, by using composite profiles made of steel and concrete (or reinforced concrete), more suitable sections can be obtained, and the required capacity increase can be achieved. However, if only moment-resisting frames (MRF) are used for design during the behavior of seismic loads, it is important to limit the relative story translations and secondary effects (López-Barraza et al. 2016). In this case, by using composite columns in the design, the required rigidity can be provided more effectively than steel and reinforced concrete systems. On the other hand, considering the large axial force strengths specified in the columns used in steel frames with central braces and eccentric braces, the required strength can be easily obtained by forming CFST columns (Etli and Güneyisi 2020a, 2020b, 2021a; Güneyisi and Etli 2021)

The use of composite profiles instead of reinforced concrete or steel profiles in high-rise designs is more advantageous in terms of construction speed and economy, especially in elements with high compressive strength, which can withstand increased axial pressures during construction and with high ductility. element design. It is known that the steel profile creates a continuous wrapping effect on the concrete in CFST column elements. On the other hand, it is expected that the strength and ductility of concrete will increase while CFST acts as a core within the element. In addition to all these positive effects, its location in the concrete core prevents regional buckling of the steel profile (Denavit et al. 2014a; Etli 2021a; Naseri and Behfarnia 2018).

It is important to examine the nonlinear responses of earthquake resistant MRF systems, in which composite section elements are used in the design phase, in terms of evaluating the advantages provided by such systems. Non-linear analyzes were used in the studies on the design and performance evaluation of multi-story MRF, which consists of composite section column and beam elements, under the influence of earthquakes. In addition, it has been seen that modeling techniques are important in studies where the natural vibration period properties of the steel-concrete composite frame and its non-linear behavior under the effect of earthquakes are examined by static and dynamic analysis (Aksoylu, C., Mobark, A., Arslan, M. H., Erkan 2020; Forcael, E., González, V., Opazo, A., Orozco, F., Araya 2020; Güler, E., Afacan 2021; Zona, Barbato, and Conte 2008).

Modeling techniques of section elements in composite element modeling can be modeled with very close results compared to experimental results when the finite element method is applied in element-based studies. On the other hand, the modeling and analysis process of these elements is quite long compared to the structural system and element properties examined. For this reason, the fiber section model, which is an alternative to this technique and provides the opportunity to make sensitive analyzes as well as being faster, seems to be a more practical method and is recommended by researchers. (Tsai et al. 2004; Vatansever and Şimşek 2021).

Many studies show that severe earthquakes are the main design factor on the structural safety of composite moment-resisting frames (CMRF) (Denavit et al. 2014b; Hajjar 2002; Lu et al. 2019; Nethercot and Vidalis 2015). One of the studies using inelastic analysis of CMRFs dates back about 30 years. They conducted a study based on CMRF designed using reinforced concrete columns and steel beams. After that, the computer program designed with developing technology and software focuses on the analysis of systems consisting of encased composite columns and composite slab steel beams. These programs were developed to analyze two-dimensional composite frames. It was formulated using the fiber element model during the modeling of the elements and the analysis of the column elements (Nethercot and Vidalis 2015). On the other hand, studies in the literature have evaluated that composite column-steel beam connections have significant effects on design and seismic performance characteristics. After examining the structures with various composite column and steel beam connection details on these effects experimentally, studies were carried out to examine theoretically (Liew et al. 2000; Xiao, Choo, and Nethercot 1996; Yang et al. 2022). In addition, theoretical and experimental investigations on the change of natural frequencies that will occur on the carrier system due to possible damage to the connection points have been carried out by the researchers (Nasery, Hüsem, Okur, Altunışık, et al. 2020; Nasery, Hüsem, Okur, and Altunişik 2020a, 2020b).

The study basically consists of two parts. In the first part, the design of CMRFs and in the second part, the performance evaluation of CMRFs were made. In stage one, the structural system consisting of composite beams made of IPE steel beams and square section CFST columns (SHS) which is assumed to be in full interaction with the slab was investigated. During the design, a point where Turkey's North Anatolian and East Anatolian fault lines intersect was considered. The parameters to be used in the seismic design of this region were selected using the interactive earthquake map. Using these parameters 5-, 10-, 15- and 20-storey CMRF structures were designed. Designs were made according to the seismic design provisions using the Regulation on the Design, Calculation and Construction Principles of Steel Structures (ÇYTHYE 2018) and the Turkish Building Earthquake Code 2018 (TBEC 2018). In the second stage, the CMRF system was remodeled for performance analysis. At this stage, the element sections were remodeled as fiber sections on an element-by-element basis using appropriate material models. Then, static pushover analysis (PO) and incremental dynamic analysis (IDA) were used to obtain information about the earthquake performance of the buildings. PO and IDA analyze were shown as generally accepted analysis tools in the literature as a very accurate structural performance value calculation tool when the correct material selection and correct element models are used (Lee and Ma 2021; Nguyen and Kim 2014; Pilarska and Maleska 2021). IDA is an emerging analysis method that offers the ability to predict seismic demand and capacity using a set of nonlinear dynamic analyzes under a multi-scale time history package. While two different lateral loading configurations were used for PO, 16 different earthquake records of selected severe earthquakes around the relevant region were used in the IDA analysis. Various parameters were evaluated for CMRFs with different properties by using the obtained graphics and design parameters. A flowchart of the method followed is presented in the Figure 1.

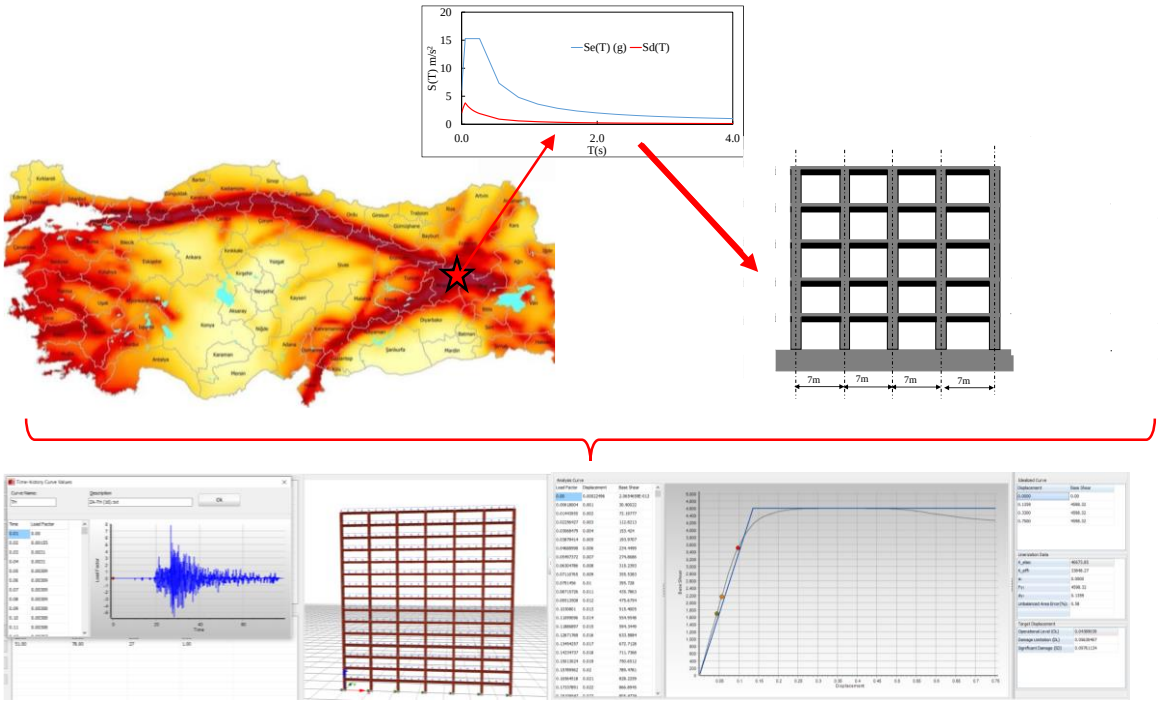

Figure 1. Flowchart of methodology.

2. Example structures

The structural element properties of the designed CMRF buildings are summarized below. The columns of the building are composite columns of CFST section obtained by filling the cores of SHS steel pipe members with concrete. Elements were dimensioned in the analyzes made under the effect of lateral earthquake loads after the preliminary design under vertical loads. Beams (with IPE steel section) and columns (with SHS section) are dimensioned using appropriate section members. In all CMRF systems, it is assumed that the frame beams are connected to the columns in a way that transmits moment. The floor slabs are designed to consist of a cast-in-place reinforced concrete slab system supported on main beams. The columns

are fixed to the foundation in both directions. The total height of the CMRF structures from the ground is modeled as 13.25, 26.5, 39.75 and 53 m for 5-, 10-, 15- and 20-storey structures, respectively. The model buildings have a floor height of 2.65 m. The model building consists of 4 openings in the x and y directions, and each span is included in the calculations as 7m. In this case, the total width is 28 m in the x and y directions (Figure 2). The use of low and medium-rise buildings is designed to be used in examining the change of system properties, as in many other studies in the literature (Denavit et al. 2014b, 2016a; Etli 2021b; Etli and Güneyisi 2020c, 2021b; Hajjar 2002; Judd and Pakwan 2018a; Nethercot and Vidalis 2015; Silva et al. 2016a; Skalomenos, Hatzigeorgiou, and Beskos 2015a). Considering the region covered in this study, the regional worst possible earthquake scenario problem is discussed. The worst ground conditions and the lowest material capacities and the design situation were considered. Basically, the possible results of the solution of this problem were tried to be examined. The CMRFs are positioned as if they were to be constructed at a location with known ground values (Latitude: 39.298011° Longitude: 41.014378°) in Bingöl Province Kaliova District Yeşilyurt Mahallesi so that earthquake parameters can be selected during the design phase. In this geographical location, data compatible with ZE ground conditions, which are the worst possible ground conditions according to the scenario in question, were considered. While the steel class is S235 in the structural elements, the concrete class is determined as C30 in the design. The analysis properties of materials were given in Table 1. SeismoStruct (SeismoSoft 2018) computer software was used in the design and performance evaluation and development of the analytical model (Figure 3).

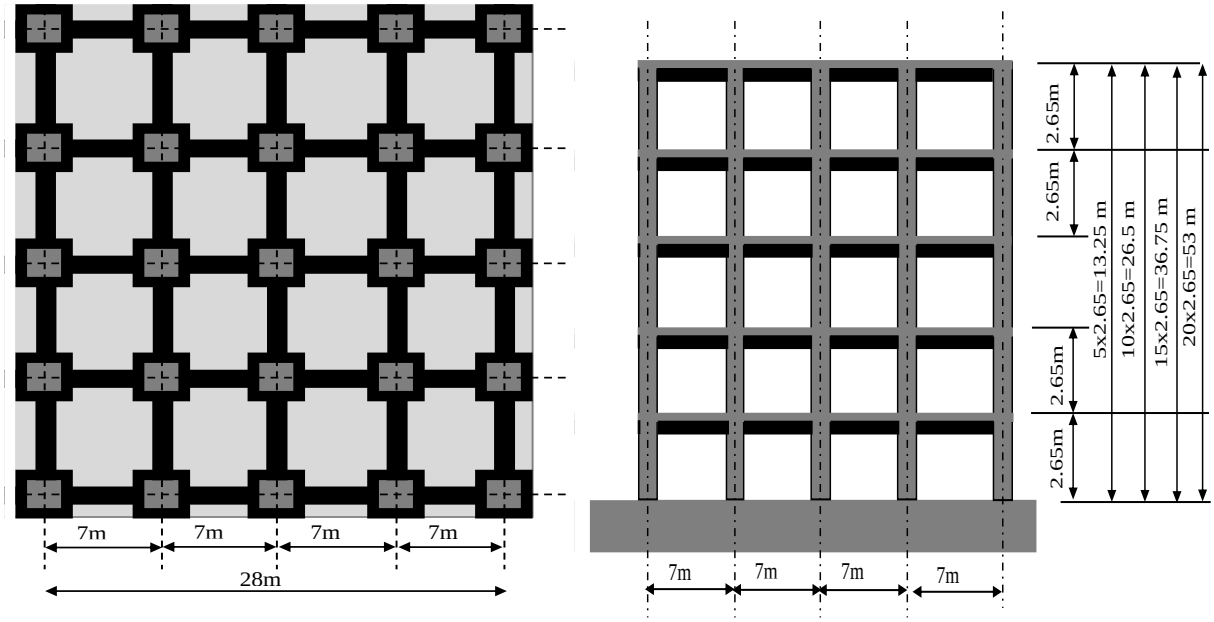

Figure 2. Schematic view of plane and elevation view.

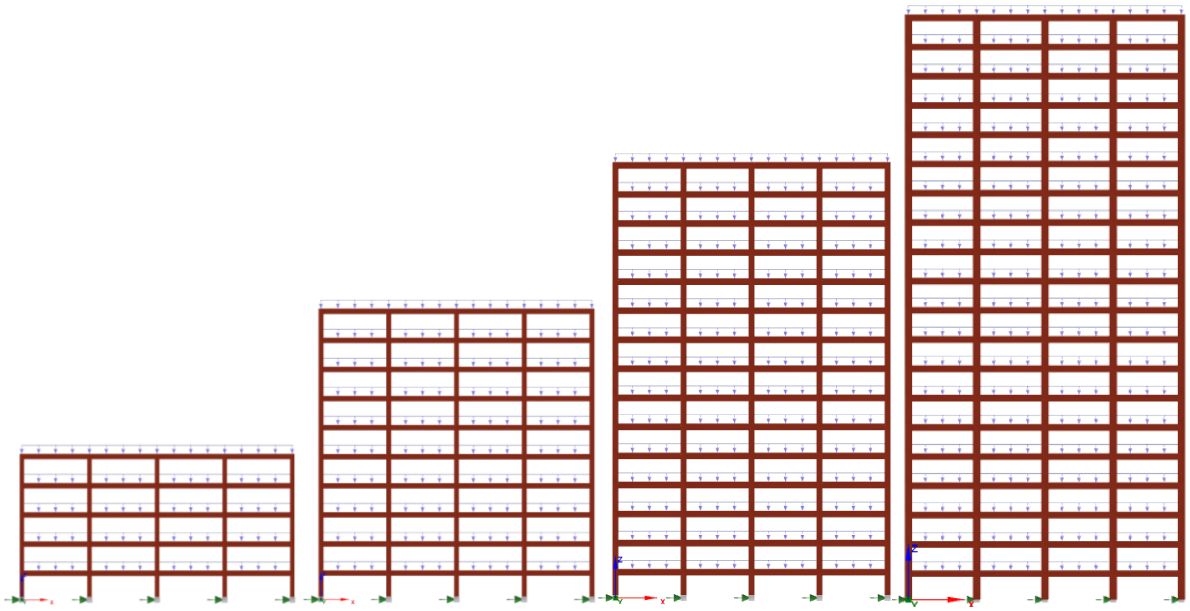

Figure 3. SeismoStruct program view of CMRFs.

2.1. *Structural design*

Table 1. Properties of materials.

	Material	
Material properties	Concrete	Steel
Compressive strength (MPa)	30	---
Yield strength (MPa)	---	235
Modulus of elasticity (GPa)	25.74	210
Strain at peak stress mm/mm	0.0022	----
Fracture/buckling strain	---	0.20
Strain hardening parameter	---	0.005
Model	con_ma	stl_bl

ÇYTHYE-2016 (ÇYTHYE 2018) and TBEC 2018 (TBEC 2018) Regulations were used in dimensioning the sections of beam and column elements that make up the CMRF system. Sections with sufficient capacity were selected by using the gravitational and seismic force values obtained from the SeismoStruct computer software. The dead weights of the CMRF system elements were calculated by the computer software and were automatically considered in the analysis. The total fixed load caused by other elements (flooring, etc.) in buildings is taken as 3 kN/m^2. The live load selected according to the purpose of use on the ground is taken as 2 kN/m^2. While the elastic design spectral accelerations used to determine the earthquake loads of the design were found, the natural vibration period was calculated using the TBEC 2018 Equation (2.2). In the creation of the horizontal elastic earthquake design spectrum, earthquake ground motion at the DD-2 levels, which has a 10% probability of exceeding in 50 years, and the local soil class ZE at the location to be constructed were used. Elastic design spectrum was obtained by using the relevant values for ZE. It is necessary to obtain the spectral acceleration coefficients and ground effect coefficients to be used in the creation of the horizontal elastic design spectrum. For this reason, a hypothetical location was chosen for the designed building. Spectral acceleration values were determined from interactive earthquake maps by using Turkey Earthquake Hazard Maps (TEHM) (Turkey Disaster and Emergency Management Presidency 2020) for this selected geographical location of the model structure. Local ground effect coefficients were obtained based on local ground class and local ground effect coefficients for the short period region and local ground effect coefficients for the 1.0 second period according to TBEC 2018 Section 2.3.3. The damping ratio values are estimated based on experience from similar structures. While these values are generally between 0.01 and 0.1 in civil engineering, the generally accepted default value of

0.05 is widely used in earthquake engineering (Elghazouli 2016; Elnashai and Sarno 2016). The damping ratio was taken as 5%. Using the TEHM, the short period map spectral acceleration coefficient was read as SS= 1.947, the map spectral acceleration coefficient for the 1.0 second period was read as $S1$= 0.514. The highest ground acceleration was obtained as PGA=0.791g and the highest ground velocity as PGV=60.469 cm/s.

As a feature of the designed CMRF systems, it was decided to create CFST columns and composite beams with high ductility. Accordingly, for the steel structure systems given in TBEC 2018 Section 4.3.2.2, the values of the CMRF system were determined by choosing the behavior coefficient R and the overstrength coefficient D. In these conditions, the coefficients of R=8 and D=3 given in this table will be taken as basis, since the entire design consists of steel-concrete composite element frames with high ductility, designed as CMRF according to TBEC 2018 Table 4.1. for earthquake effects. The General Analysis Method was used to calculate the required strength of the building elements against the design earthquake forces affecting the CMRF system, and the Design Method with Load and Strength Coefficients was used in the dimensioning phase. As a requirement of this method, all elements in the structural system (composite columns and frame beams in this example) are multiplied by an axial and shear stiffness coefficient. This value to be used in ÇYTHYE 6.2.3 is given as 0.8. The reduction coefficient applied to the bending stiffnesses of the composite columns was obtained as 0.8x0.8 = 0.64 as stated in ÇYTHYE 6.2.3(b) and 12.2.5(d).

As a result of the seismic design analyzes made with SeismoStruct (SeismoSoft 2018) computer software, the natural vibration periods for 5-, 10-, 15- and 20-storey structures were obtained by the program as 0.720, 1.430, 1.642 and 2.110s, respectively. Total CMRF weights were obtained from the software as 5108.91, 10892.29, 18597.46 and 26434.289 kN for 5-, 10-, 15- and 20-storey structures, respectively. In the seismic design calculations for 5-storey, 10-storey, 15-storey and 20-storey structures, the base shear forces of 583.9, 644.92, 932,924 and 1010.278 kN were calculated from the software, respectively. The results of the analysis and the smooth geometry of the system showed that the system did not contain any irregularities in the plan and in the vertical, which should be evaluated under the effect of earthquakes. In seismic design, effective relative story drifts and second order effects are evaluated using limit values. These limit values were calculated as lower than the limit values defined in TBEC 2018 clause 4.9 for CMRFs designed during seismic analysis. Columns were sized according to the conditions specified in ÇYTHYE 2016 12.3.2 by using the internal force values of the elements calculated with the design loads obtained. Table 12.5 is given to obtain the axial force-bending moment interaction diagram of the column section in ÇYTHYE and the plastic stress distribution method for it. In addition, according to the condition given in TBEC 2018 9.11.4.2, the axial compressive force values in all composite columns must meet the condition $N_{dm} \leq 0.40 P_{no}$.

While calculating the N_{dm} value, the joint effect of vertical loads and earthquake loads is considered. In addition, live load reduction coefficients defined in TS 498 (TS-498 2007) are used for live loads in these calculations. Consequently, N_{dm} is defined as the largest of the axial compression forces calculated using the specified live load reduction coefficients. P_{no} is defined as the compressive strength of the cross section of the composite element under axial load. During the design of CMRFs, according to TBEC 2018 article 9.11.2.2, in the calculations made by considering the earthquake direction in all directions, the columns should have higher strength than the beams at all column-beam junction points in the structure. In 5-, 10-, 15- and 20-storey CMRF structures, CFST composite columns (outside diameter × wall thickness) formed from 450×16, 500×36, 600×45 and 750×45 mm SHS section steel tube elements were used as elements. After the static and dynamic design, the steel beam sections in composite beams were calculated as IPE 400 for 5 and 10 story structures and as IPE 500 for 15 and 20 story structures. Reinforced concrete slab thicknesses were measured as 150 mm in buildings with 5 and 10 floors, and 180 mm in buildings with 15 and 20 floors. Moreover, the building plan geometry, material and modeling properties were created by evaluating previous studies (Tsai et al. 2004; Vatansever and Şimşek 2021). The results of the mode shapes from the natural vibrations obtained from the software during the seismic design are presented in the Figure 4.

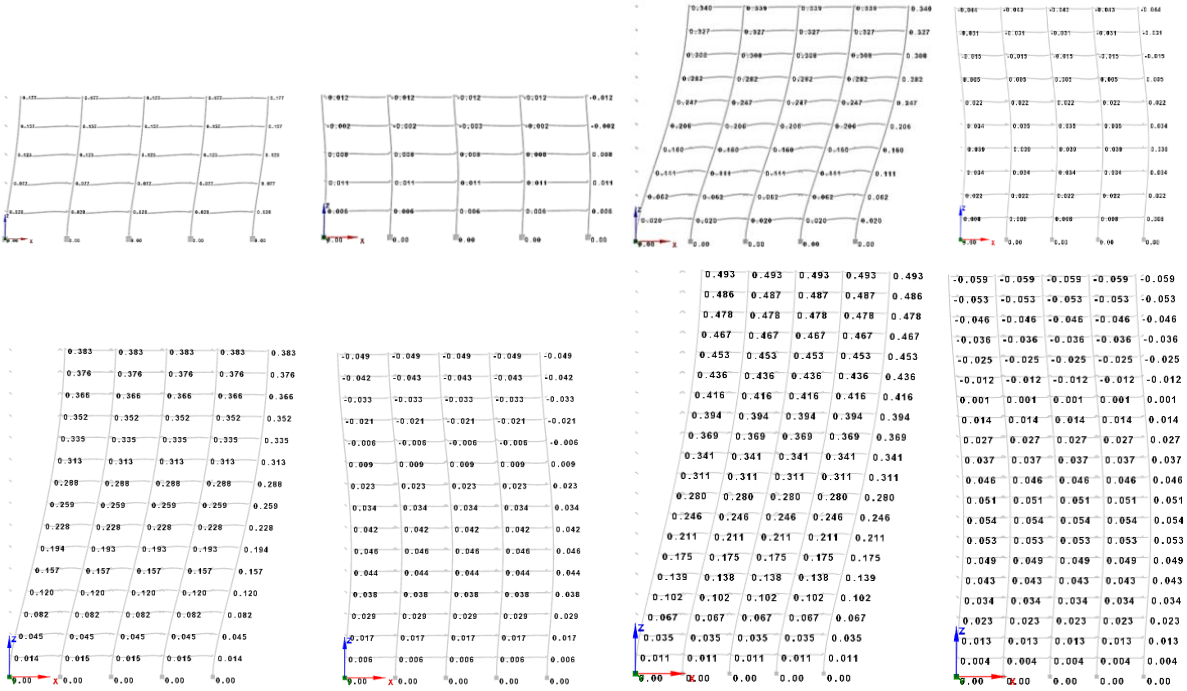

Figure 4. First two mode shape from natural vibrations taken from SeismoStruct program.

2.2. *Nonlinear analytical models of the CMRF system*

In the first stage, CMRFs were designed statically and dynamically according to ÇYTHYE 2016 Regulation and TBEC 2018, and then the results of their nonlinear behavior were evaluated using analytical models using SeismoStruct computer software. For this, structural and geometric quadratic effects were considered in all analyzes made in the software, especially in a non-linear manner. In the evaluation of performances, all results obtained with PO and IDA in CMRF buildings were evaluated comparatively for different parameters. In the new models produced to evaluate the behavior of CMRFs, elements with a distributed plastic behavior approach were selected from the software for the nonlinear behavior of columns and beams. For this reason, a section that reflects the plastic behavior of beams and columns was chosen in the model. This section model is one in which the fiber-shaped section model (Figure 5) is used, which ensures that solutions are as accurate and fast as possible. In this model, it is assumed that the plastic behavior spreads to the transverse and longitudinal sections formed in the section with the help of fibers. Moreover, the fiber section modeling used in the designed elements provides a relatively accurate description of the section behavior against the combined load effect. The cross-sectional stress-strain state enables the integration of nonlinear uniaxial material response of individual fibers that subdivides the sections by the algorithm in the program's artificial intelligence. This software considers the spread of behavior between fiber elements along the section depth at regular intervals along the element length (SeismoSoft 2018). Accordingly, the cross-sections of beams and columns in these regions consist of a finite number of fiber elements. More importantly, it is assumed that full adherence is provided between the concrete and steel section parts that make up the composite section. The plastic behavior in these regions is determined directly by the SeismoStruct software based on material properties. Slabs are not directly included in the analytical models but are assumed to form rigid diaphragms in each floor plane. The vertical loads passing through the floors are defined as the loads of the frame beams, and the evenly distributed loads are defined as the loads. Calibrations of element material models and behavior models were obtained from previous studies (Etli 2021c, 2022; Etli and Güneyisi 2020d, 2021c, 2022b, 2022a; Güneyisi and Etli 2020).

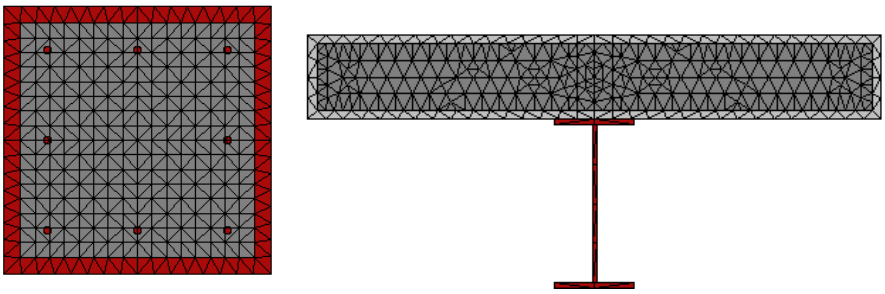

(a) (b)

Figure 5. Fiberized section views for (a) CFST columns and (b) composite beam.

The expected material strength values defined in TBEC 2018 were used to describe the performances of steel and concrete materials used in CMRF elements in nonlinear behavior models. The data in TBEC 2018 Table 5.1 was used to obtain the values of these expected material strengths. For these values, $1.3fck$ and $1.5Fy$ formulations were used, respectively, while reaching the expected material strengths in the characteristic compressive strength of concrete and the characteristic yield strengths for S235 class structural steel. In the model used for nonlinear material behavior in PO and IDA analyzes of steel material, a hardening-based coefficient of 0.005 is used. In the SeismoStruct software, the bilinear steel model was used to model the structural steel material in nonlinear analysis. This material model is defined in the software as the "stl_bl" material model. During the PO and IDA analyzes of the concrete material, the tensile strength was neglected in the stress-strain material response curve. In addition, while the concrete behavior of the CMRF models is modeled in the SeismoStruct software, the "con_ma" model in the software is used for the non-linear behavior of the material. Each of the IDAs, consisting of nonlinear analyzes in the time domain (TH), is performed using pre-occurring and locally selected earthquake ground motions that move simultaneously in a vertical horizontal plane under the influence of a constant gravitational load. While calculating the gravitational load values, 30% of the live load values are added to the weight of the building in addition to the fixed loads that are effective in an earthquake. performance evaluation analysis consists of two parts. In the first step, PO analyzes were used. In these analyses, two different loading conditions were evaluated. These loads were used as uniformly distributed horizontal loading (ULD-PO) and triangular horizontal loading (TLD-PO). In the second stage, IDA analyzes were performed. The earthquake ground motions selected for this purpose consist of 8 ground motion pairs. When selecting earthquakes, large-scale earthquakes that occurred in the past between the North Anatolian fault line and the East Anatolian fault line surrounding the city of Karlıova, which is assumed to have been built, were used (Figure 6).

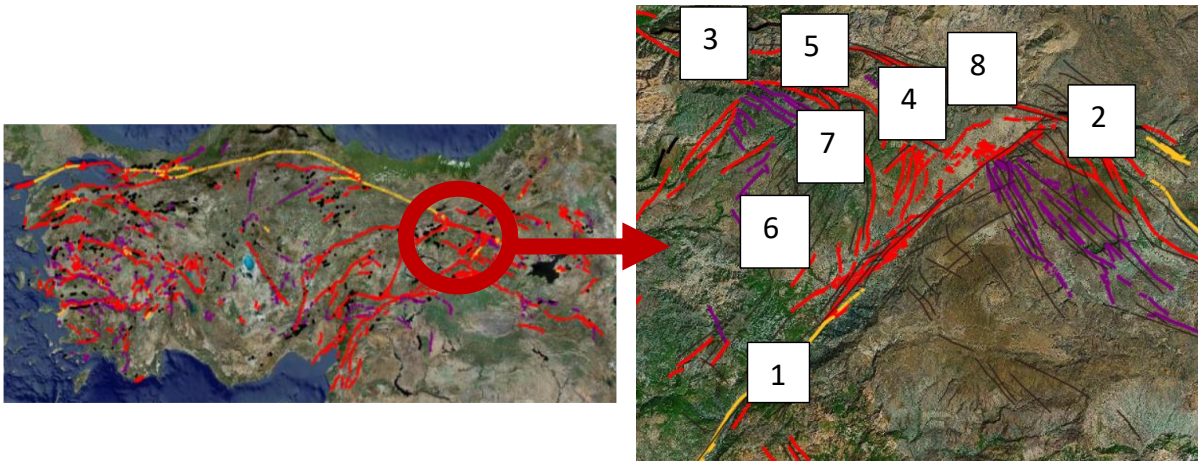

Figure 6. Selected ground motion schematic representation.

The multipliers used to increase TH values in IDA analyzes were chosen as 0.05, 0.10, 0.20, 0.30, 0.40, 0.50, 0.60, 0.80, 1.00, 1.20, 1.40, 1.50, 1.75, 2.00, 2.30, 2.60, 2.90, 3.20, 3.50, 3.80, and 4.00. It is aimed that the total number of IDA analyzes

will be 8x2=16. Seismic demand values and other parameters are calculated by taking the average of the values obtained because of 16 IDA analyzes. The characteristics of the earthquake records used in the study within the scope of RIA are presented in Table 2. The data and information regarding the earthquake movements in Table 2 were taken from the AFAD ground motion database (TADAS 2021). Using existing earthquake records, each selected ground motion pair was scaled and used in IDA analyzes with the aid of an earthquake spectrum, defined in the study as a design earthquake for CMRFs and evaluated using a 475-year return period with a 10% probability of exceedance in 50 years.

After severe earthquakes, especially in earthquakes such as the Kahramanmaraş earthquake, two earthquakes of 7.8 Mw and 7.5 Mw in the Pazarcık and Ekinözü districts of Kahramanmaraş, the designs of the structures to be built on weakly graded soils are of great importance. It is important to put the information in current regulations into practice and to evaluate engineering. Therefore, within the scope of the study, possible uses of current building systems were evaluated in terms of superstructure. The structures produced are especially evaluated as residential structures. In addition, the general building coefficients used in such structures were considered. After the data obtained, it was tried to produce information and data about the design-performance change that would provide a preliminary idea to the designer.

Table 2. Properties of earthquake ground motions.

Record ID	Record Seq. #	Station ID	Epicentral Distance (km)	Event Depth (km)	ML/MW	Ø
TH-1 TH-2	2183	1133	11.8	6	6.6/-	E W
TH-3 TH-4	2896	1206	2.19	15.8	5.1/-	E W
TH-5 TH-6	23	2402	12.82	23	6.1/-	E W
TH-7 TH-8	10099	1212	16.2	8	-/5.7	E W
TH-9 TH-10	24	2402	45.32	29	5.4/-	E W
TH-11 TH-12	1828	2306	30.88	15.51	-/5.2	E W
TH-13 TH-14	6027	6202	37	10.66	-/5.3	E W
TH-15 TH-16	2587	1208	54.09	9.9	5.4/-	E W

*Ø: Component

3. Results and discussion

The response of CMRFs because of ULD-PO and TLD-PO analysis is shown in Figure 7. In the graphs given, the horizontal axis is the ratio of the roof displacement to the building height, and the vertical axis is the ratio of the base shear to the building weight. In 5-story CMRFs, IDA analysis presents a behavior that lies between the first-mode dominant response and the higher-mode response. However, on the other hand, the IDA results obtained in 10-, 15- and 20-storey structures are parallel to the ULD-PO results, so it can be said that higher modes dominate in these structures (Etli and Güneyisi 2020b, 2020a, 2021a; Turkey Disaster and Emergency Management Presidency 2020; Vamvatsikos 2005, 2015; Vamvatsikos and Allin Cornell 2002). The IDA was performed by using selected TH records to obtain the seismic response of the case study CMRFs. The dynamic behavior of the structures is also plotted in Figure 7.

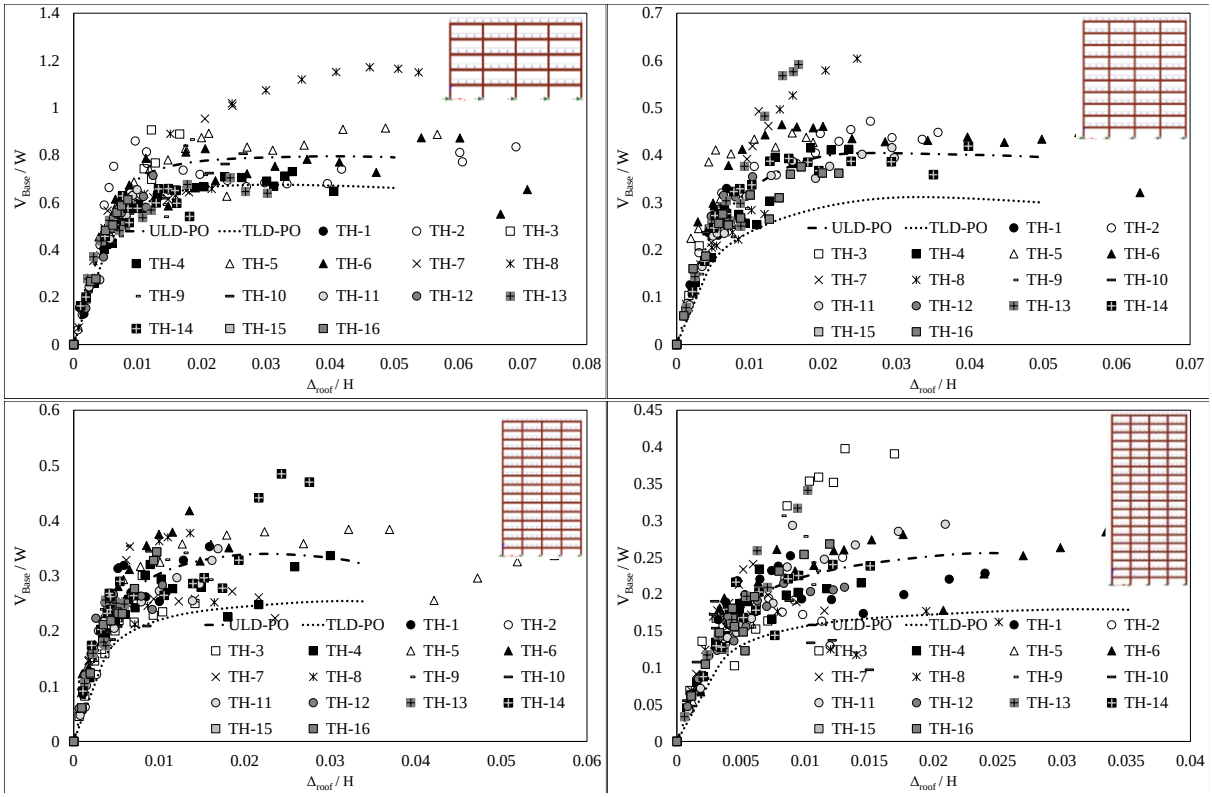

Figure 7. PO and IDA graphs for CMRF structures a) 5, b) 10, c) 15, and d) 20 stories.

3.1. *Ductility factor*

In the literature are examined, it is used to express the degree of inelastic deformations that occur due to earthquake ground motion under the influence of a structural system or a horizontal load that it may be exposed to while calculating the ductility ratio (Miranda and Bertero 1994). That is, the displacement ductility ratio μ (ductility demand) can be expressed as:

$$\mu = \frac{\Delta_u}{\Delta_y} \quad (1)$$

Yield and ultimate displacement values are Δ_y and Δ_u, respectively, in Equation (1). As a result of IDAs, it was calculated from Fig. 5 and the data were calculated and plotted for average value of μ. μ factors were calculated from IDA, TLD-PO, and ULD-PO for 5-, 10-, 15- and 20-story CMRF structures and given in Figure 6. If the μ values obtained because of the IDA are examined, it is calculated as 2.03, 1.96, 2.65 and 3.19 for the buildings with 5-, 10-, 15- and 20-story, respectively. When the μ results are examined, the values obtained because of TLD-PO are lower than the values obtained from IDA by 12.82%, 24.40% and 34.98% for 10-, 15- and 20-story buildings, respectively. However, the μ values obtained because of TLD-PO in the 5-story structure are 4.33% higher than the values obtained from IDA. When the μ values obtained because of ULD-PO were examined, it was found that for 10-, 15- and 20-storey structures, they were 10.32%, 18.60% and 28.25% lower, respectively, then those obtained from IDA. In the 5-storey building, the difference between the μ values calculated from IDA and the μ values obtained because of ULD-PO is negligible (0.55%) Figure 8.

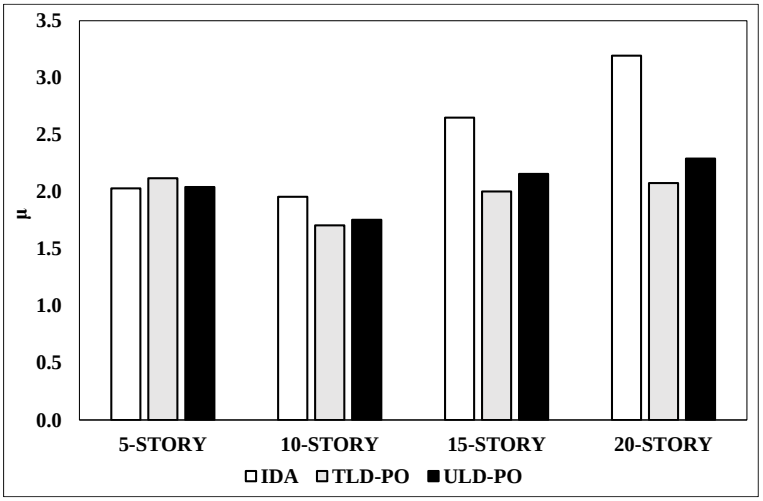

Figure 8. Ductility factor for CMRFs.

3.2. Overstrength factor

When describing the nonlinear response of structures, the load-displacement relationship is often assumed to be elasto-plastic. Within the scope of this study, the structural extreme strength factors expressed by the following equation were calculated from the Figs. obtained with IDAs for each structure:

$$\Omega_d = \frac{V_y}{V_d} \quad (2)$$

Yield and design base shear values are displayed as V_y and V_d, respectively, in Equation (2). As a result of experimental and theoretical studies conducted by researchers for Ω_d, an important performance parameter of the building, it has been shown that this factor plays an important role in protecting buildings from collapse in the face of severe earthquakes (Elnashai et al. 2002; Elnashai and Di Sarno 2015; Whittaker, Hart, and Rojahn 1999). It has been reported in the literature that this factor for steel and reinforced concrete structures varies between 1.8 and 6.5 for long-term and short-term structures (Elnashai and Di Sarno 2015).

In this study, IDA results showed that the Ω_d factors of CMRFs reached 6.66, 7.13, 6.48 and 5.87 in 5-, 10-, 15- and 20-story structures, respectively. Ω_d factors obtained from TLD-PO analyzes are 1.91%, 1.01% and 7.97% higher for 5-, 15- and 20-storey buildings, respectively, than those obtained from IDA. In the 10-story structure, the Ω_d factor for TLD-PO is 8.09% smaller than the values obtained from IDA. For ULD-PO, it is 12.44%, 32.27%, 26.28% and 24.36% lower than the Ωd factors calculated from IDA for 5-, 10-, 15- and 20-story buildings, respectively (Figure 9).

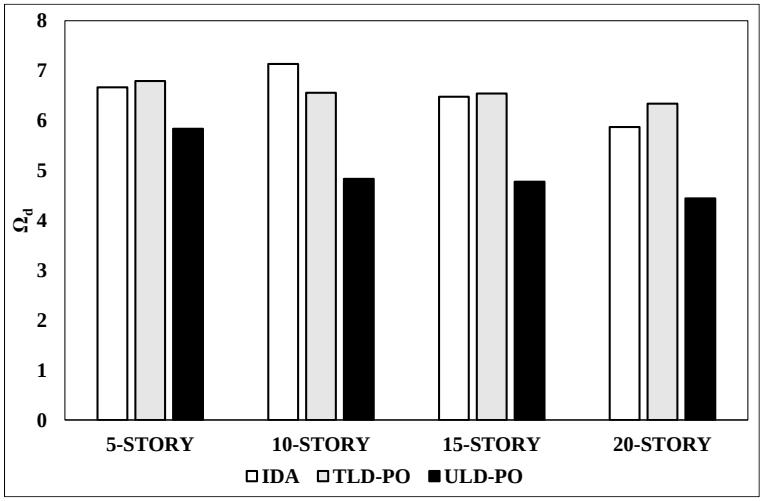

Figure 9. Overstrengh factor for CMRFs.

3.3. Inherent overstrength factor

Elnashai and Mwafy (Elnashai and Mwafy 2002) recently suggested a measure of response termed 'inherent overstrength factor. Inherent overstrength factor (Ω_i) is formulated as below.

$$\Omega_i = \frac{V_y}{V_e} \quad (3)$$

Yield and elastic base shear values are given as V_y and V_e, respectively, in Equation (3). The suggested measure of response Ω_i reflects the reserve strength and the anticipated behavior of the structure under the design earthquake. Clearly, in the case of $\Omega_i \geq 1.0$, the global response will be almost elastic under the design earthquake, reflecting the high overstrength of the structure. If $\Omega_i < 1.0$, the difference between the value of Ω_i and unity is an indication of the ratio of the forces that are imposed on the structure in the post-elastic range (Elnashai and Di Sarno 2015). When the values obtained within the scope of the study were examined, the values of the Ω_i parameter were obtained as 0.85, 0.90, 0.81 and 0.73 from the IDA results for 5-, 10-, 15- and 20-story CMRF, respectively. These values show that the structures can survive the earthquakes with inflexible deformations. Considering the analyzes made with TLD-PO, the calculated Ω_i values were 1.91%, 1.01% and 7.97% greater than the IDA results for the 5-, 15- and 20-story CMRF, respectively. On the other hand, according to the IDA results, the Ω_i value is 8.09% smaller in 10-story building. On the other hand, ULD-PO results were 12.44%, 32.27%, 26.28% and 24.36% smaller than IDA results for 5, 10, 15 and 20-story CMRF, respectively (Figure 10).

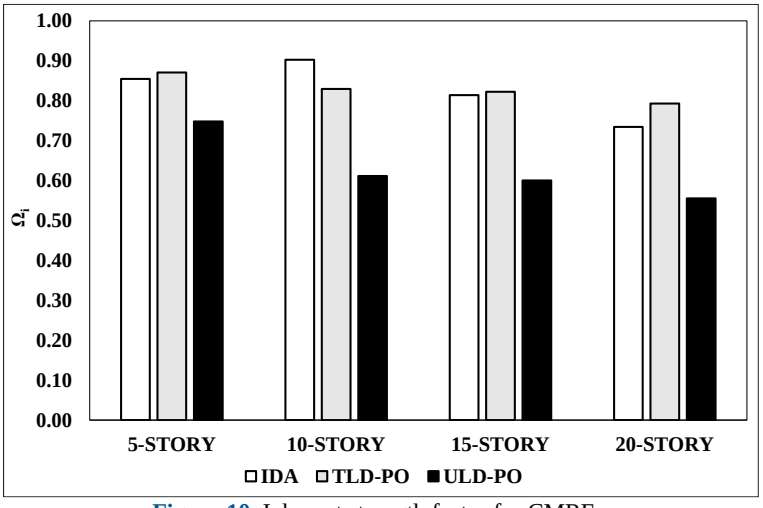

Figure 10. Inherent strength factor for CMRFs.

3.4. Composite section capacities

In this part of the paper, the examination of the deformations in the structural elements because of the non-linear dynamic and static analyzes carried out in the systems formed by the CMRF structures is presented. The deformation states and definitions that occur in the mentioned structural elements are summarized in Table 3. The deformations in the CFST column cross sections in the CMRF system and in the sections of the composite beams, which are formed by the combination of IPE section and solid slab, are examined within the scope of this section. During the examination, IDR (interstory drift ratio) values were taken into consideration. The cross-sectional deformations obtained during IDA, TLD-PO and ULD-PO given in the Table 3 were evaluated. When the results of IDA, TLD-PO and ULD-PO analyzes are examined, the deformation limits of CSY, CSU, CCU and CCF in CFST elements in CMRF systems are examined, and limit states of BSY, BSU, BCU and BCF deformations in composite beams are examined.

Table 3. Deformation states and definitions.

Abbreviations	Definition
BSY	In the composite beam, the steel has reached yield elongation at the outermost fiber
CSY	In the composite column, the steel has reached yield elongation at the outermost fiber.
BSU	Steel reached its ultimate capacity in the composite beam.
CSU	Steel reached its ultimate capacity in the composite column.
BCU	Concrete reached its ultimate capacity in the composite beam.
CCU	Concrete reached its ultimate capacity in the composite column.
BCF	In the composite beam, the concrete converged to the elongation at crushing limit.
CCF	In the composite column, the concrete converged to the elongation at crushing limit.

In the IDA analysis, when the IDR value reaches 0.0072, 0.0067, 0.0052 and 0.0044 in 5-, 10-, 15- and 20-storey structures, respectively, BSY deformation in composite beams is at limit values. On the other hand, the IDR value at which BSY deformations occur in ULD-PO analyzes is 10%, 15%, 13% and 3% smaller than the values calculated with IDA in 5-, 10-, 15- and 20-storey structures, respectively. In addition, the IDR values at which BSY deformations occur in TLD-PO analyzes are 15%, 13%, 11%, and 2% smaller than the values calculated with IDA for 5-, 10-, 15-, and 20-storey structures, respectively. The IDR values at which BSU deformation occurred were calculated from the IDA results as 0.0353, 0.0329, 0.0259, and 0.024 for 5-, 10-, 15-, and 20-storey structures, respectively (Figure 11).

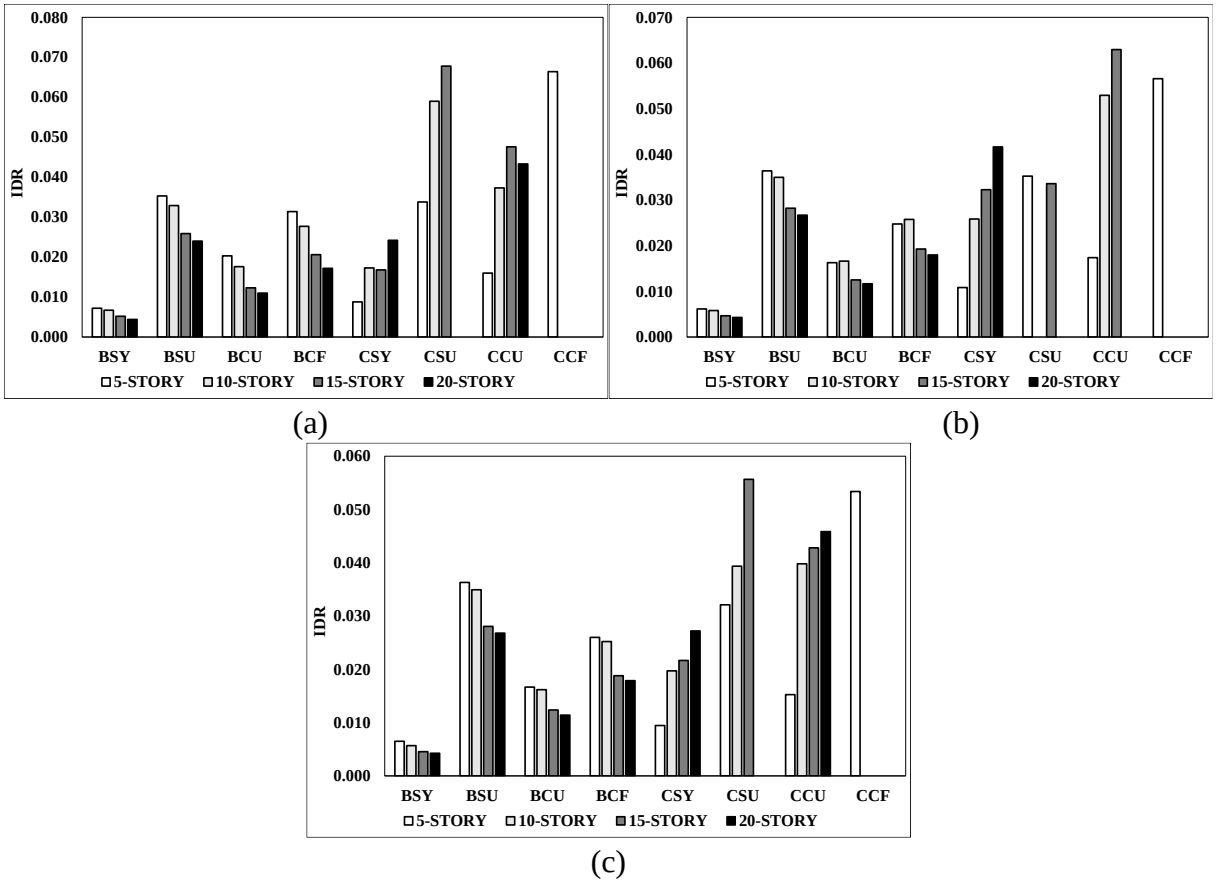

Figure 11. Section deformation variation with IDR for a) IDA, b) TLD-PO, and c) ULD-PO.

In ULD-PO analyzes, the IDR value at which BSU deformations occur was 3%, 6%, 8% and 12% greater than the values calculated with IDA in 5-, 10-, 15- and 20-storey structures, respectively. In TLD-PO analysis, the IDR value at which BSU deformations occur was 3%, 6%, 9% and 11% greater than the values calculated with IDA in 5-, 10-, 15- and 20-storey structures, respectively. Therefore, the results obtained have almost the same difference with IDA. When the BCU deformation occurring in the reinforced concrete parts of the composite beams was examined, it was observed that the IDR value reached 0.0203, 0.0176, 0.0123, and 0.011 in 5-, 10-, 15- and 20-storey structures, respectively, in IDA analyses. On the other hand, in ULD-PO analyzes, the IDR value at which this deformation occurs is 18% and 8% smaller than the values calculated with IDA for 5- and 10-storey structures, respectively.

Similarly, in TLD-PO analyzes, the IDR value at which this deformation occurs is 20% and 6% smaller than the values calculated with IDA in 5- and 10-storey structures, respectively. On the other hand, in the ULD-PO analysis, the IDR at which this deformation occurred was 1% and 4% greater than the values calculated with IDA for 15- and 20-storey buildings, respectively. Similarly, in TLD-PO analysis, the IDR at which this deformation occurred was 2% and 6% greater than the values calculated with IDA for 15- and 20-storey structures, respectively. Again, the final deformation BCF in the reinforced concrete part of the composite beams was observed when the IDR value reached 0.0314, 0.0277, 0.0206, and 0.0172 in 5-, 10-, 15- and 20-storey structures, respectively, in IDA analyses. On the other hand, the IDR value at which this deformation occurs in ULD-PO analyzes is 17%, 9%, and 9% smaller than the values calculated with IDA for 5-, 10-, and 15-storey structures, respectively. In addition, in TLD-PO analyzes, the IDR value at which this deformation occurs is 21%, 7% and 6% smaller than the values calculated with IDA for 5-, 10-, and 15-storey structures, respectively. In ULD-PO and TLD-PO analyzes, this deformation is 4% greater than the values calculated with IDA for 20-story structures (Figure 11).

Deformations occurring in CFSTs were observed as CSY, CSU, CCU, and CCF. CSY deformation in CFST is at the limit values when the IDR value in IDA analyzes reaches 0.0088, 0.0173, 0.0168 and 0.0242 values for 5-, 10-, 15- and 20-storey structures, respectively. On the other hand, the IDR value at which CSY deformations occur in ULD-PO analyzes is 7%, 14%,

29% and 12% greater than the values calculated with IDA in 5-, 10-, 15- and 20-storey structures, respectively. In addition, the IDR value at which CSY deformations occur in TLD-PO analyzes is 23%, 49%, 92%, and 72% greater than the values calculated with IDA for 5-, 10-, 15-, and 20-storey structures, respectively. The IDR values at which CSU deformation occurred were calculated from the IDA results as 0.0338, 0.059 and 0.0678 for 5-, 10- and 15-storey structures, respectively. It is not included in the results of all three analyzes in the 20-layer CMRF. In ULD-PO analyzes, the IDR value at which CSU deformations occur is 5%, 33% and 18% smaller than the values calculated with IDA in 5-, 10-, and 15-storey structures, respectively. The structures in which CSU deformations occur in TLD-PO analyzes are only 5- and 15-storey structures. For this analysis method, the IDR value is 4% greater in 5-storey buildings, respectively, than the values calculated with IDA, while it is 50% smaller in 15-storey structures (Figure 10).

The IDR values at which CCU deformation occurred were calculated from the IDA results as 0.016, 0.0373, 0.0476 and 0.0433 for 5-, 10-, 15- and 20-storey structures, respectively. In the 20-story CMRF, however, this deformation does not occur because of TLD-PO. In ULD-PO analyzes, the IDR value at which CSU deformations occur is 5% and 10% smaller than the values calculated with IDA for 5- and 15-storey structures, respectively. In addition, the IDR at which CSU deformations occur in ULD-PO analyzes is 7% and 6% greater than the values calculated with IDA for 10- and 20-storey structures, respectively. In TLD-PO analysis, CCU deformations are 9%, 42%, and 32% larger than the values calculated by IDA in 5-, 10- and 15-storey structures. CCF deformation, on the other hand, occurred only in the 5-story structure for all three analyses. For this case, it was observed that the IDR values for IDA, ULD-PO and TLD-PO were 0.0664, 0.0534 and 0.0566, respectively (Figure 11).

4. Conclusions

In this study, if the structures designed according to ÇYTHYE 2016 and TBEC 2018 design codes are built on specific design conditions, deformations in the sections of the elements and various performance parameters are obtained. By using these parameters, the mutual performance changes of the structures were evaluated. Static pushover analysis and incremental dynamic analysis were performed to determine performance parameters. Two different lateral loading models were used for static pushover and analyzes consisting of 16 earthquake records were used for IDA analysis. In addition, in the next step of the research, studies have been carried out to provide more reliable information to the designer by making models similar to international codes, developing soil structure integration models and updating the analyzes. The following conclusions can be reached for the structural systems whose data have been examined:

1. Ductility factor, μ values greater than 1.7 were obtained. This shows that CMRF structures can adequately absorb system displacements and earthquake effects thanks to their lateral mobility and element ductility. On the other hand, this value is evaluated according to the structural system in Eurocode-8 [60]. In CMRF systems it is obtained on average 30% larger than given in Eurocode-8.
2. The Ω_d parameter calculated due to the IDA caused by the regional earthquakes selected for the buildings designed as CMRF was obtained as the lowest 5.87 and the highest 7.13. In the PO analysis, the lowest value is 4.44 and the highest value is 6.79. While the Ω_d parameter obtained from the IDA results increased in low-rise and mid-rise buildings, a decreasing trend was observed as the number of stories increased. In PO analysis, on the other hand, as the number of stories increases, the value of the Ω_d parameter decreases.
3. In Ω_i values, all values are calculated less than 1. In this case, structures absorb the earthquake energy thanks to their inelastic behavior under severe earthquakes. This is also supported by the deformation limit results in the section on member section deformations occurring in the elements.
4. According to the change in the IDR of the deformations in the composite beams, when the IDR value is 0.005, it is seen that the section behavior is within the elastic limits. On the other hand, when the IDR value is above 0.02, the plastic behavior in the sections of composite beams dominates the behavior of the structure. However, this situation emerges as a decreasing IDR value as the number of floors increases.
5. When the IDR value in the CFST columns in the carrier system is 0.009, it can be said that the section behavior is within elastic limits. When the IDR value is 0.03 and above, it is seen that plastic behavior comes to the fore in CFST column sections. This situation emerges as an increasing IDR value as the number of floors increases.

Funding: Not applicable.

Conflicts of interest: The author would like to declare that the author does not have any potential conflict of interest regarding this research.

References

Aksoylu, C., Mobark, A., Arslan, M. H., Erkan, İbrahim H. 2020. "A Comparative Study on ASCE 7-16, TBEC-2018 and TEC-2007 for Reinforced Concrete Buildings." *Revista De La Construcción. Journal of Construction* 19(2):282–305.

ÇYTHYE. 2018. "Calculation and Construction Principles of Steel Structures."

Denavit, Mark D., Jerome F. Hajjar, Roberto T. Leon, and Tiziano Perea. 2014a. "Analysis and Design of Steel-Concrete Composite Frame Systems." Pp. 2605–16 in *Structures Congress 2014 - Proceedings of the 2014 Structures Congress*.

Denavit, Mark D., Jerome F. Hajjar, Tiziano Perea, and Roberto T. Leon. 2016. "Seismic Performance Factors for Moment Frames with Steel-concrete Composite Columns and Steel Beams." *Earthquake Engineering & Structural Dynamics* 45(10):1685–1703. doi: 10.1002/eqe.2737.

Elghazouli, A. Y. Y., J. M. M. Castro, and B. A. A. Izzuddin. 2008. "Seismic Performance of Composite Moment-Resisting Frames." *Engineering Structures* 30(7)(7):1802–19. doi: 10.1016/j.engstruct.2007.12.004.

Elghazouli, Ahmed. 2016. *Seismic Design of Buildings to Eurocode 8*. 1st ed. CRC Press.

Elnashai, A. S., and A. M. Mwafy. 2002. "Overstrength and Force Reduction Factors of Multistorey Reinforced-Concrete Buildings." *The Structural Design of Tall Buildings* 11(5):329–51.

Elnashai, A. S., A. M. Mwafy, A. S. Elnashai, A. M. Mwafy, A. S. Elnashai, and A. M. Mwafy. 2002. "Overstrength and Force Reduction Factors of Multistorey Reinforced-Concrete Buildings." *Structural Design of Tall Buildings* 11(5):329–51.

Elnashai, A. S., and L. Di Sarno. 2015. *Fundamentals of Earthquake Engineering: From Source to Fragility, 2nd Edition*. John Wiley & Sons.

Elnashai, Amr, and Luigi Di Sarno. 2016. *Fundamentals of Earthquake Engineering: From Source to Fragility*. 1st ed. John Wiley & Sons.

Etli, Serkan. 2021a. "Analytical Evaluation of Behavior of Composite Columns Under Axial Load." *International Journal of Pure and Applied Sciences*. doi: 10.29132/ijpas.991166.

Etli, Serkan. 2022. "Parametric Analysis of the Performance of Steel-Concrete Composite Structures Designed with TBDY 2018." *International Journal of Innovative Engineering Applications* 6(1). doi: 10.46460/ijiea.1029942.

Etli, Serkan, and Esra Mete Güneyisi. 2020a. "Response of Steel Buildings under near and Far Field Earthquakes." *Civil Engineering Beyond Limits* 1(2):24–30. doi: 10.36937/cebel.2020.002.004.

Etli, Serkan, and Esra Mete Güneyisi. 2020b. "Seismic Performance Evaluation of Regular and Irregular Composite Moment Resisting Frames." *Latin American Journal of Solids and Structures* 17(7):1–22. doi: 10.1590/1679-78255969.

Etli, Serkan, and Esra Mete Güneyisi. 2021a. "Assessment of Seismic Behavior Factor of Code-Designed Steel–Concrete Composite Buildings." *Arabian Journal for Science and Engineering* 46(5):4271–92. doi: 10.1007/s13369-020-04913-9.

Etli, Serkan, and Esra Mete Güneyisi. 2022a. "Effect of Nonlinear Modeling Approaches Used for Composite Elements on Seismic Behavior of Composite Framed Buildings." *Sadhana - Academy Proceedings in Engineering Sciences* 47(2). doi: 10.1007/s12046-022-01871-w.

Etli, Serkan, and Esra Mete Güneyisi. 2022b. "Effect of Using Eccentric Braces with Different Link Lengths on the Seismic Demand of CFST Column-Composite Beam Frames Subjected to Near-Field and Far-Field Earthquakes." *Iranian Journal of Science and Technology - Transactions of Civil Engineering*.

Forcael, E., González, V., Opazo, A., Orozco, F., Araya, R. 2020. "Modeling the Performance Impacts Caused by an Earthquake to the Construction Industry: Case Study on the 2010 Chile Earthquake." *Revista De La Construcción. Journal of Construction* 16(2):215–228.

Güler, E., Afacan, K. B. 2021. "Assessment of Shear Wave Velocity Concept on the Site Specific Analysis and Its Effects over Performances of Building Codes." *Revista De La Construcción. Journal of Construction* 20(3):527–543.

Güneyisi, Esra Mete, and Serkan Etli. 2020. "Response of Steel Buildings under near and Far Field Earthquakes." *Civil Engineering Beyond Limits* 1(2):24–30. doi: 10.36937/cebel.2020.002.004.

Güneyisi, Esra Mete, and Serkan Etli. 2021. "Investigation of the Effect of Diagonal Eccentricity on Behavior of Braced Composite Structures Under the Impact of Near and Far-Field Earthquakes." *TUBİTAK* PROJECT NO.

Hajjar, Jerome F. 2002. "Composite Steel and Concrete Structural Systems for Seismic Engineering." *Journal of Constructional Steel Research* 58(5–8):703–23. doi: 10.1016/S0143-974X(01)00093-1.

Judd, Johnn P., and Nipun Pakwan. 2018. "Seismic Performance of Steel Moment Frame Office Buildings with Square Concrete-Filled Steel Tube Gravity Columns." *Engineering Structures* 172:41–54. doi: 10.1016/j.engstruct.2018.06.016.

Khosravi, H., Shoaib Mousavi, S., Tadayonfar, G. 2020. "Numerical Study of Seismic Behavior of Composite Steel Plate Shear Walls with Flat and Corrugated Plates." *Evista De La Construcción. Journal of Construction* 16(2):249–260.

Lee, Shu-Chi, and Chau-Khun Ma. 2021. "Time History Shaking Table Test and Seismic Performance Analysis of Industrialised Building System (IBS) Block House Subsystems." *Journal of Building Engineering* 34:101906. doi: 10.1016/j.jobe.2020.101906.

Liew, J. Y. Richard, T. H. Teo, N. E. Shanmugam, and C. H. Yu. 2000. "Testing of Steel–Concrete Composite Connections and Appraisal of Results." *Journal of Constructional Steel Research* 56(2):117–50. doi: 10.1016/S0143-974X(99)00099-1.

López-Barraza, Arturo, Sonia E. Ruiz, Alfredo Reyes-Salazar, and Edén Bojórquez. 2016. "Demands and Distribution of Hysteretic Energy in Moment Resistant Self-Centering Steel Frames." *Steel and Composite Structures* 20(5):1155–71. doi: 10.12989/scs.2016.20.5.1155.

Lu, Xinzheng, Lei Zhang, Kaiqi Lin, and Yi Li. 2019. "Improvement to Composite Frame Systems for Seismic and Progressive Collapse Resistance." *Engineering Structures* 186:227–42. doi: 10.1016/j.engstruct.2019.02.006.

Miranda, Eduardo, and Vitelmo V. Bertero. 1994. "Evaluation of Strength Reduction Factors for Earthquake-Resistant Design." *Earthquake Spectra* 10(2):357–79. doi: 10.1193/1.1585778.

Naseri, Reza, and Kiachehr Behfarnia. 2018. "A Numerical Study on the Seismic Behavior of a Composite Shear Wall." *Computers and Concrete* 22(3):279–89. doi: 10.12989/cac.2018.22.3.279.

Nasery, Mohammad Manzoor, Metin Hüsem, Fatih Yesevi Okur, and Ahmet Can Altunişik. 2020a. "Damage Effect on Experimental Modal Parameters of Haunch Strengthened Concrete-Encased Composite Column–Beam Connections." *International Journal of Damage Mechanics* 29(2):297–334. doi: 10.1177/1056789519843330.

Nasery, Mohammad Manzoor, Metin Hüsem, Fatih Yesevi Okur, and Ahmet Can Altunişik. 2020b. "Numerical and Experimental Investigation on Dynamic Characteristic Changes of Encased Steel Profile Before and After Cyclic Loading Tests." *International Journal of Civil Engineering* 18(12):1411–31. doi: 10.1007/s40999-020-00545-0.

Nasery, Mohammad Manzoor, Metin Hüsem, Fatih Yesevi Okur, Ahmet Can Altunışık, and Mohammad Emran Nasery. 2020. "Model Updating-based Automated Damage Detection of Concrete-encased Composite Column-beam Connections." *Structural Control and Health Monitoring* 27(10). doi: 10.1002/stc.2600.

Nethercot, David, and Carolos Vidalis. 2015. "Improving the Resistance to Progressive Collapse of Steel and Composite Moment Frames." Pp. 1138–49 in *Structures Congress 2015*. Reston, VA: American Society of Civil Engineers.

Nguyen, Phu-Cuong, and Seung-Eock Kim. 2014. "Nonlinear Inelastic Time-History Analysis of Three-Dimensional Semi-Rigid Steel Frames." *Journal of Constructional Steel Research* 101:192–206. doi: 10.1016/j.jcsr.2014.05.009.

Pilarska, Dominika, and Tomasz Maleska. 2021. "Numerical Analysis of Steel Geodesic Dome under Seismic Excitations." *Materials* 14(16):4493. doi: 10.3390/ma14164493.

SeismoSoft. 2018. "SeismoStruct: A Computer Software for Static and Dynamic Nonlinear Analysis of Framed Structures."

Shams, Mohammad, and M. Ala Saadeghvaziri. 1997. "State of the Art of Concrete-Filled Steel Tubular Columns." *ACI Structural Journal* 94(5):558–71. doi: 10.14359/505.

Shanmugam, N. E., and B. Lakshmi. 2001. "State of the Art Report on Steel-Concrete Composite Columns." *Journal of Constructional Steel Research* 57(10):1041–80. doi: 10.1016/S0143-974X(01)00021-9.

Silva, A., Y. Jiang, L. Macedo, J. M. Castro, R. Monteiro, and N. Silvestre. 2016. "Seismic Performance of Composite Moment-Resisting Frames Achieved with Sustainable CFST Members." *Frontiers of Structural and Civil Engineering* 10(3):312–32. doi: 10.1007/s11709-016-0345-y.

Skalomenos, Konstantinos A., George D. Hatzigeorgiou, and Dimitri E. Beskos. 2015. "Seismic Behavior of Composite Steel/Concrete MRFs: Deformation Assessment and Behavior Factors." *Bulletin of Earthquake Engineering* 13(12):3871–96. doi: 10.1007/s10518-015-9794-2.

TADAS. 2021. "Turkey Acceleration Database and Analysis System (TADAS)." *Https://Tadas.Afad.Gov.Tr/Map*.

TBEC. 2018. "Turkish Building Earthquake Code 2019." *Resmi Gazete, No: 30364 (Mükerrer)*.

TS-498. 2007. "Yapı Elemanlarının Boyutlandırılmasında Alınacak Yüklerin Hesap Değerleri." *Türk Standartları Enstitüsü*.

Tsai, K. C., J. W. Lai, C. H. Chen, B. C. Hsiao, Y. T. Weng, and M. L. Lin. 2004. "Pseudo Dynamic Tests of a Full Scale CFT/BRB Composite Frame." *Proceedings of the 2004 Structures Congress - Building on the Past: Securing the Future* 1241–50. doi: 10.1061/40700(2004)131.

Turkey Disaster and Emergency Management Presidency. 2020. "Turkey Earthquake Hazard Maps." *Https://Tdth.Afad.Gov.Tr/*. Retrieved (https://tdth.afad.gov.tr/).

Vamvatsikos, Dimitrios. 2005. "Seismic Performance, Capacity and Reliability of Structures as Seen Through Incremental Dynamic Analysis."

Vamvatsikos, Dimitrios. 2015. "Incremental Dynamic Analysis." *Encyclopedia of Earthquake Engineering* 1165–71. doi: 10.1007/978-3-642-35344-4_136.

Vamvatsikos, Dimitrios, and C. Allin Cornell. 2002. "Incremental Dynamic Analysis." *Earthquake Engineering and Structural Dynamics* 31(3):491–514. doi: 10.1002/eqe.141.

Vatansever, Cüneyt, and Yunus Emre Şimşek. 2021. "Design and Nonlinear Time History Analysis of a Multi-Story Building with Concrete Filled Composite Columns and Steel Beams." *Pamukkale University Journal of Engineering Sciences* 27(3):264–73. doi: 10.5505/pajes.2020.91043.

Whittaker, Andrew, Gary Hart, and Christopher Rojahn. 1999. "Seismic Response Modification Factors." *Journal of Structural Engineering* 125(4):438–44.

Xiao, Y., B. S. Choo, and D. A. Nethercot. 1996. "Composite Connections in Steel and Concrete. Part 2 — Moment Capacity of End Plate Beam to Column Connections." *Journal of Constructional Steel Research* 37(1):63–90. doi: 10.1016/0143-974X(95)00015-N.

Yang, Il-Seung, Deuckhang Lee, Hyunjin Ju, Se-Jung Lee, and Jae-Yuel Oh. 2022. "Steel-Concrete Composite Beam-Column Connections Utilizing Pre-fabricated Permanent Steel Form." *Journal of Building Engineering* 46:103836. doi: 10.1016/j.jobe.2021.103836.

Zona, Alessandro, Michele Barbato, and Joel P. Conte. 2008. "Nonlinear Seismic Response Analysis of Steel–Concrete Composite Frames." *Journal of Structural Engineering* 134(6):986–97. doi: 10.1061/(ASCE)0733-9445(2008)134:6(986).